

Radial Basis Function Neural Network for Electrochemical Impedance Prediction at Presence of Corrosion Inhibitor

Hossein Komijani^{1*}, Sepideh Rezaei Hassanabadi²,
Mohammad Reza Parsaei³, Saeed Maleki⁴

Received 06 April 2016; accepted after revision 09 August 2016

Abstract

Simulation and preparing predictive model of electrochemical impedance Nyquist plots based on radial basis function neural network (RBFNN) are presented in this paper. The RBFNN as a powerful predictive system predicts the real and imaginary parts of impedance as a function of time, temperature and inhibitor concentration. The mean R value of 0.9996 as regression coefficient and mean square error (MSE) value of 1.72×10^{-3} as results show the validity of proposed method for simulation and prediction of electrochemical impedance spectroscopy (EIS) in different environmental situations.

Keywords

electrochemical impedance, radial basis function neural network, corrosion inhibitor, simulation

1 Introduction

One of the serious problem in oil and gas production technology is corrosion that mainly occurred by carbon dioxide (CO_2) as sweet corrosion and/or hydrogen sulfide (H_2S) as sour corrosion in water injection system [1]. The usage of inhibitors in oil industry is currently prevalent because of the effectiveness and low cost such as nitrogen based inhibitors [2]. The adsorption ability depends on the sort of corrosion environment, the kind and surface of metal and inhibitor chemical structure [3]. Many studies are performed recently to model the experimental corrosion data. Artificial neural network (ANN) is used to predict metal corrosion manner in [4]. The issue of whitening environment on pitting corrosion is analyzed in [5].

The electrochemical impedance spectroscopy (EIS) is an approach to investigate the metal kinetic and electrodeposition information. One of the most relevant techniques to obtain this information is the simulation of the system impedance [6]. The multi-layer perceptron (MLP) is used to simulate and to plot the electrochemical impedance spectroscopy diagram in [6] and [7]. In [7], the steel EIS in a corrosive environment is studied considering the corrosion inhibitor concentrations as 5 and 25 ppm, and two MLPs are trained separately according to each of these corrosion inhibitor concentration database. Inputs of MLPs were time and real part of impedance and the output of MLPs was the imaginary part of impedance. Thus, it can be deduced that the imaginary part of impedance was defined as a function of time and real part of impedance as:

$$Z_{im} = f(t, Z_{re}) \quad (1)$$

where Z_{im} imaginary part of impedance, Z_{re} is the real part of impedance, t is the time of experiment and f was a function that was approximated by MLP.

In our study, Z_{im} and Z_{re} are both selected as outputs, because they depend on the experiment conditions, and the independent parameters such as temperature, corrosion inhibitor concentration and lapse of experiment time are selected as inputs of the simulation system. So, it can be written:

$$[Z_{im}, Z_{re}] = f(t, T, c) \quad (2)$$

¹ Faculty of Electrical and Computer Engineering,
University of Tabriz, Tabriz, Iran

² Faculty of Electrical Engineering, Ghasosodin Jamshid Kashani Higher
Education Institute, Ghazvin, Iran

³ Department of Computer Engineering and Information Technology,
Shiraz University of Technology, Shiraz, Iran

⁴ Faculty of Chemical and Petroleum Engineering,
University of Tabriz, Tabriz, Iran

*Corresponding author, e-mail: h.komijani90@ms.tabrizu.ac.ir

where t is the time of experiment, c is the concentration of corrosion inhibitor and f is a function that is approximated by radial basis function neural network (RBFNN).

In this paper, a new automatic model based on RBFNN is presented to predict various chemical impedance spectroscopy from different inhibitor concentrations and different experiment temperatures during the time in an environment including NaCl and CO₂ to resemble crude oil and transport industries environments.

RBFNN is a special class of single hidden layer feedforward neural network for application to problems of supervised learning. Supervised learning is interpreted as estimating a function from some input-output pairs with little or no knowledge of the form of the function. RBFNN is a technique to approximate function that trained by couples of input-output to implement interpolation [8-10]. RBFNNs are capable of approximating well any function [11]. In this paper, the mean of utilizing RBFNN is to estimate the underlying EIS function and to estimate its output at certain desired values of the input.

In corrosion surveys, electrochemical impedance spectroscopy is a method that use alternating current (AC) exerted over an electrode to gain relevant responds. According to Ohm's laws, the relation between voltage (V) and current (I) expresses as follow:

$$V = RI \quad (3)$$

where R is resistance. Equation (3) alters to (4) in case of AC signals:

$$V = ZI \quad (4)$$

where Z is total impedance that composes of real part as resistance (R), and imaginary part as reactance (X):

$$Z = R + jX \quad (5)$$

The amount of X depends on applied signal frequency. Equation (5) would be rephrased to (6) according to our case study [7]:

$$Z = R + jX = R_s + \frac{R_{ct}}{1 + jwC_{dl}R_{ct}} \quad (6)$$

where w is the applied signal frequency, R_s is resistance, R_{ct} and C_{dl} are the electrochemical double layer or charge transfer resistance and capacitance respectively. Theoretically, typical Nyquist plot would be a semicircle [12].

2 Material and Method

2.1 Experimental Database

The experimental database was prepared in Faculty of Chemical and Petroleum Engineering, University of Tabriz. The material used in the experiments was carbon steel manganese with its main chemical composition as vanadium 0.001 wt.%, niobium 0.055 wt.%, and titanium 0.014 wt.%.

The size of pieces was 0.030×0.30×0.010 m. Samples were heated at 1250 °C at a heating rate of 0.4 °C/s, drenched for 90 min. Then, the rolling stage is performed immediately from 1250 °C to 1098 °C in five steps, reaching 42.3% of total deformation hot rolled and an average strain rate of 2.48 s⁻¹. Then, a cooling stage ending at 867 °C, achieving a total deformation of 37% in five steps with an average strain rate of 2.98 s⁻¹ is performed. The samples were cooled again by forced nitrogen gas to 650 °C. After that, the samples were left to be cool to the ambience temperature. The pieces were polished using 600 grit SIC emery paper and then cleaned with alcohol, acetone, and distilled water. The commercial carboxyamidoimidazoline dissolved in pure 2-propanol was used as inhibitor in this study. The inhibitor was mixed to a solution of 3% NaCl, heated, deaerated by Nitrogen gas and CO₂-saturated for 120 minutes pre-prepared, continues bubbling and seething during the experiments. The experiments were carried out using signals adjusted by the amplitude of 10 mV and the frequency of 0.1 Hz to 100 KHz applied with a model PC4 300 Gamry potentiostat at the free corrosion potential during 11 hours. Electrochemical impedance spectroscopy tests were carried out at the free corrosion potential.

2.2 Radial basis function neural network (RBFNN) architecture

RBFNN were originally developed for exact interpolation of a set of data points in multidimensional space. The aim of exact interpolation is to project every input vector x_i , onto the corresponding target y_i , to find a function $f(x)$ such that:

$$y_i = f(x_i) \quad (7)$$

where $i = 1, \dots, m$, m is the number of objects. According to the radial basis function approach, exact mapping can be performed using a set of m basis functions (one for each data point) with the form $\phi(\|x_i - x_j\|)$, where $\phi(\cdot)$ is some non-linear function, and $\|\cdot\|$ denotes distance between x_i and x_j , usually Euclidean distance. Then the output of the mapping can be presented as linear combinations of these basis functions:

$$y_i = f(x_i) = \sum_{j=1:m} w_j \phi(\|x_i - x_j\|) \quad (8)$$

where w_j denotes weights, x_i and x_j are input object and center of basis function respectively. The basis functions can have different forms. The most popular among them is Gaussian function:

$$\phi(\|x_i - x_j\|) = \exp\left(-\frac{\|x_i - x_j\|^2}{2\sigma^2}\right) \quad (9)$$

where σ is controlling the smoothing properties of the interpolating function [13].

RBFNN can be presented as a three-layer feedforward structure as shown in Fig. 1. The input layer serves only as input distributor to the hidden layer. Each node in the hidden layer

is a radial function as dimensionality being the same as the dimensionality of the input data. The output is calculated by a linear combination i.e. a weighted sum of the radial basis function according to (8) [13].

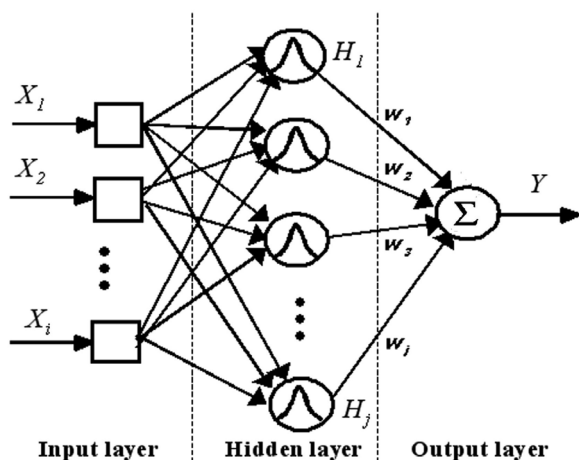


Fig. 1 Radial basis function neural network (RBFNN)

It is easy to determine an equation for obtaining the weights of network by converting (8) to the matrix format as:

$$Y = W\Phi \quad (10)$$

where $Y = \{y_i\}$, $W = \{w_j\}$ and $\Phi = \{\phi(\|x_i - x_j\|)\}$. Then, W matrix is gained by:

$$W = Y\Phi^{-1} \quad (11)$$

where Φ^{-1} is calculated by pseudo inverse as:

$$\Phi^{-1} = (\Phi^T \Phi)^{-1} \Phi^T \quad (12)$$

where Φ^T is the conjugate transpose of Φ .

The RBFNN is configured and implemented in Matlab software. The network has three inputs and two outputs as the inputs are time in minute (min), temperature in centigrade ($^{\circ}\text{C}$) and concentration of inhibitor in gram per liter (g/l), whereas

the outputs are real and imaginary parts of impedance in ohm square centimeter.

3 Results and Discussion

The experimental database was separated to two parts of train part (80% of database) and test part (20% of database). The RBFNN was trained with the train part, then the provided RBFNN was tested with the test part and the results of the prediction are shown in Fig. 2, Fig. 4 and Fig. 6.

Experimental condition of inhibitor concentration of 10^{-3} at temperature 25°C , inhibitor concentration of 3×10^{-5} at temperature 45°C and inhibitor concentration of 5×10^{-4} at temperature 65°C are selected as samples and the prediction results are shown in Fig. 2, Fig. 4 and Fig. 6 respectively. According to the Fig. 2, Fig. 4 and Fig. 6, it is obvious that the proposed RBFNN can show high performance in predicting electrochemical impedance values with negligible error. The nugatory error indicates that the developed RBFNN technique performs superlatively in regard of predicting electrochemical impedance. The mean square error (MSE) is expressed as:

$$MSE = \frac{1}{M} \sum_{k=1}^M [x_k - \hat{x}_k]^2 \quad (13)$$

where M is the length of signal. The MSE of predictions for Fig. 2, Fig. 4 and Fig. 6 are calculated as $MSE = 7.66 \times 10^{-4}$, $MSE = 3.89 \times 10^{-4}$ and $MSE = 1.16 \times 10^{-4}$ respectively, and the mean MSE for all database was obtained as $Mean. MSE = 1.72 \times 10^{-3}$.

The regression performance of selected sample experimental conditions are shown in Fig. 3, Fig. 5 and Fig. 7 respectively. The regression coefficients of $R=0.99991$, $R=0.99983$ and $R=0.99976$ were obtained for these figures respectively, and the mean regression coefficient for all database was obtained as $Mean.R=0.99966$, which indicate the high ability of proposed RBFNN for corrosion modeling and predicting studies and can determine different impedance behaviors in various conditions confidently.

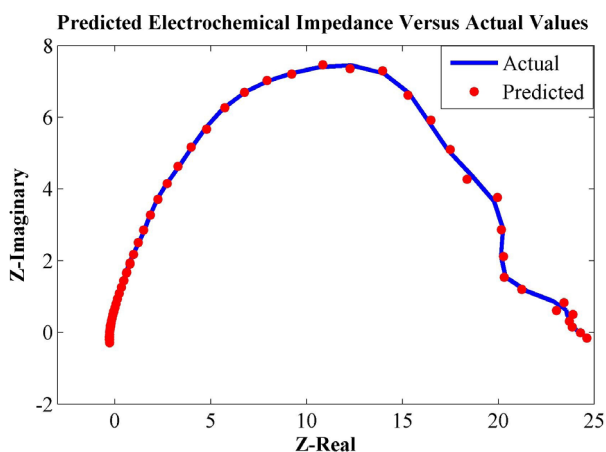


Fig. 2 Predicted electrochemical impedance against actual values in inhibitor concentration of 10^{-3} at temperature 25°C

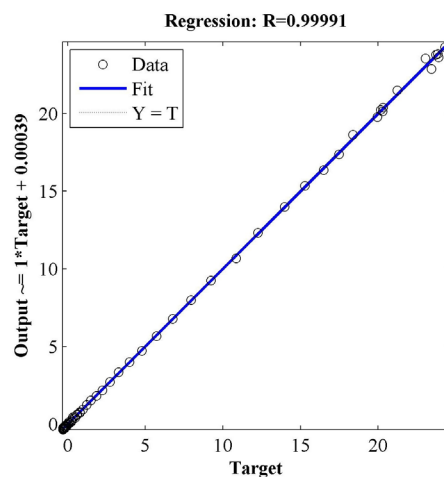


Fig. 3 Regression performance of predicted and actual values of electrochemical impedance in inhibitor concentration of 10^{-3} at temperature 25°C

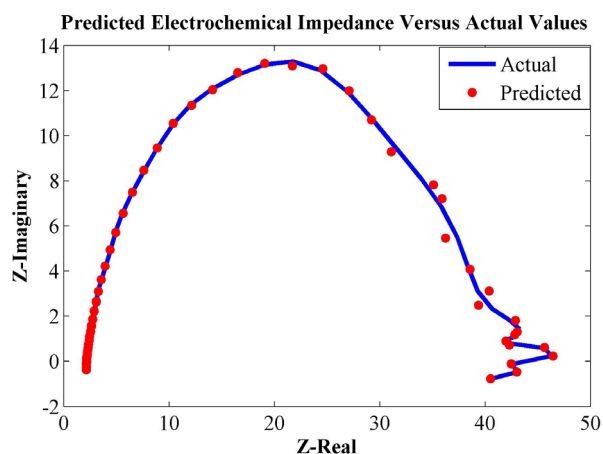


Fig. 4 Predicted electrochemical impedance against actual values in inhibitor concentration of 3×10^{-5} at temperature 45°C .

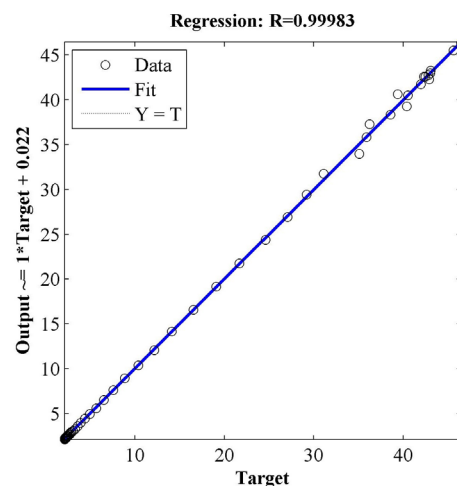


Fig. 5 Regression performance of predicted and actual values of electrochemical impedance in inhibitor concentration of 3×10^{-5} at temperature 45°C .

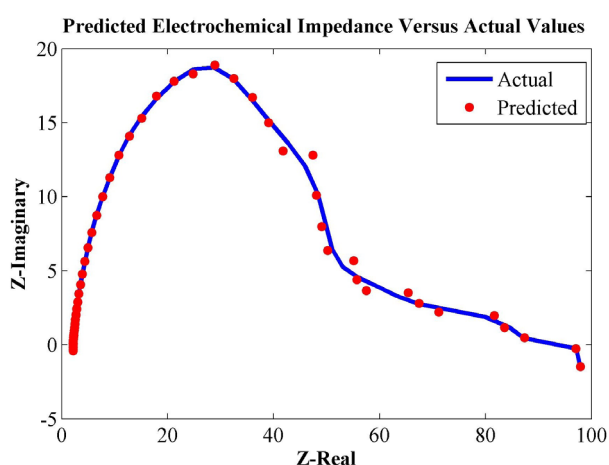


Fig. 6 Predicted electrochemical impedance against actual values in inhibitor concentration of 5×10^{-4} at temperature 65°C

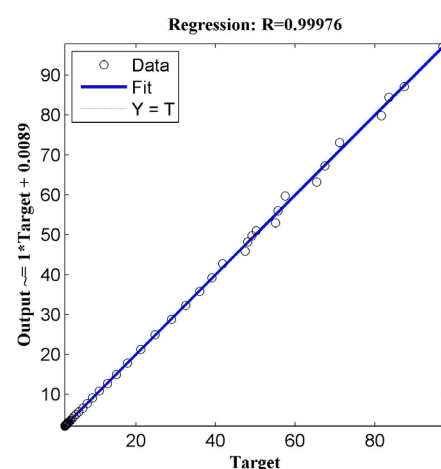


Fig. 7 Regression performance of predicted and actual values of electrochemical impedance in inhibitor concentration of 5×10^{-4} at temperature 65°C

4 Conclusions

This paper presents a **radial basis function neural network (RBFNN) prediction and modeling of electrochemical impedance under various conditions such as different inhibitor concentrations, different temperatures during the time**. The RBFNN can perform sufficiently with negligible error of prediction. This method can be utilized in modeling, predicting, Nyquist plotting and estimating the electrochemical impedance, corrosion resistance of diverse materials over the wide range of situations. The productivity in this sort of modeling is related to the fact that the developed technique do not need any suppositions in advance on the **underlying corrosion type or chemical mechanisms**.

References

- [1] Kermani, M. B., Morshed, A. "Carbon Dioxide Corrosion in Oil and Gas Production—A Compendium." *Corrosion*. 59(8), pp. 659-683. 2003. <https://doi.org/10.5006/1.3277596>
- [2] Zhang, X., Wang, F., He, Y., Du, Y. "Study of the Inhibition Mechanism of Imidazoline Amide on CO₂ Corrosion of Armco iron." *Corrosion Science*. 43(8), pp. 1417-1431. 2001. [https://doi.org/10.1016/S0010-938X\(00\)00160-8](https://doi.org/10.1016/S0010-938X(00)00160-8)
- [3] Bentiss, F., Lagrenee, M., Traisnel, M., Hornez, J. C. "The corrosion inhibition of mild steel in acidic media by a new triazole derivative." *Corrosion Science*. 41(4), pp. 789-803. 1999. [https://doi.org/10.1016/S0010-938X\(98\)00153-X](https://doi.org/10.1016/S0010-938X(98)00153-X)
- [4] Kamrunnihar, M., Urquidí-Macdonald, M. "Prediction of corrosion behavior using neural network as a data mining tool." *Corrosion Science*. 52(3), pp. 669-677. 2010. <https://doi.org/10.1016/j.corsci.2009.10.024>
- [5] Moayed, M. H., Golestani-pour, M. "An investigation on the effect of bleaching environment on pitting corrosion and transpassive dissolution of 316 stainless steel." *Materials and Corrosion*. 56(1), pp. 39-43. 2005. <https://doi.org/10.1002/maco.200403809>

- [6] Cristea, M., Varvara, S., Muresan, I., Popescu, I. C. "Neural network approach for simulation of electrochemical diagrams." *Indian Journal of Chemistry*. 42A, pp. 764-768. 2003. URL: <http://nopr.niscair.res.in/handle/123456789/18188>
- [7] Colorado-Garrido, D., Ortega-Toledo, D. M., Hernández, J. A., González-Rodríguez, J. G., Uruchurtu, J. "Neural networks for Nyquist plots prediction during corrosion inhibition of a pipeline steel." *Journal of Solid State Electrochemistry*. 13(11), pp. 1715-1722. 2009. <https://doi.org/10.1007/s10008-008-0728-7>
- [8] Bishop, C. M. "Neural Networks for Pattern Recognition." Oxford, UK, Oxford University Press, 1995.
- [9] Buhmann, M. D., Dai, F. "Point wise approximation with quasi-interpolation by radial basis functions." *Journal of Approximation Theory*. 192, pp. 156-192. 2015. <https://doi.org/10.1016/j.jat.2014.11.005>
- [10] Izquierdo, D., de Silanes, M. C. L., Parra, M. C., Torrens, J. J. "CS-RBF interpolation of surfaces with vertical faults from scattered data." *Mathematics and Computers in Simulation*. 102, pp. 11-23. 2014. <https://doi.org/10.1016/j.matcom.2013.05.015>
- [11] Chen, T., Chen, H. "Approximation capability to functions of several variables, nonlinear functionals, and operators by radial basis function neural networks." *IEEE Transactions on Neural Networks*. 6(4), pp. 904-910. 1995. <https://doi.org/10.1109/72.392252>
- [12] Mitton, D. B., Wallace, S. L., Cantini, N. J., Bellucci, F., Thompson, G. E., Eliaz, N., Latanision, R. M. "The Correlation between Substrate Mass Loss and Electrochemical Impedance Spectroscopy Data for a Polymer-Coated Metal." *Journal of The Electrochemical Society*. 149(6), pp. B265-271. 2002. <https://doi.org/10.1149/1.1473777>
- [13] Afiatdoust, F., Esmailbeigi, M. "Optimal variable shape parameters using genetic algorithm for radial basis function approximation." *Ain Shams Engineering Journal*. 6(2), pp. 639-647. 2015. <https://doi.org/10.1016/j.asej.2014.10.019>